

Variations of muon flux in the atmosphere during thunderstorms

G. G. Karapetyan

Cosmic Ray Division, Yerevan Physics Institute, Yerevan 0036, Armenia

(Received 28 November 2013; published 5 May 2014)

The variations of muon flux that are occasionally registered by ground-based scintillation detectors during thunderstorms are investigated. The variations are mainly negative (deficit) and originate due to the electric field of thunderclouds. They last from several minutes up to several hours and demonstrate minor (up to a few percent) deviations against the background. We develop an appropriate theoretical model to describe this phenomenon by investigating the two processes responsible for it: (i) the transformation of an energetic spectrum of muons in the electric field due to their acceleration or deceleration, and (ii) the decay of muons conditioned by a short life span. The change of muon flux near the ground is derived at a given altitudinal distribution (profile) of the electric field. Two possible opposite cases of an altitudinal profile of a two-layered electric field are considered: (i) upward directed in the lower layer of the cloud and downward directed in the upper layer and (ii) vice versa. We find that in case (i), the deficit of muon fluxes is observed by the detector at any threshold energy. It emerges due to a decrease of the flux of positive muons decelerated in the lower layer of a thundercloud. The corresponding increase of the flux of accelerated muons turns out to be smaller because of their partial decaying. As a result, an uncompensated decrease of total flux of muons is formed near the ground. However, in case (ii), the deficit is smaller, and it may become positive when it is observed by detectors with a threshold energy larger than ~ 300 MeV. The results may help estimate the height and electric field of thunderclouds by analyzing the records of muon detectors with different energy thresholds.

DOI: [10.1103/PhysRevD.89.093005](https://doi.org/10.1103/PhysRevD.89.093005)

PACS numbers: 92.60.Pw, 13.40.-f, 94.05.Dd, 96.50.sb

I. INTRODUCTION

Large impulsive enhancements of the fluxes of low energy cosmic-ray particles occur occasionally during thunderstorms. These upward- and downward-directed pulses lasting from microseconds and up to dozens of minutes are intense gamma rays produced by low energy electrons in the atmosphere (see Ref. [1]). However, sometimes the opposite phenomenon—the decrease of the flux of higher energy (>100 MeV) cosmic-ray particles is observed during thunderstorms as well [2–8]. These decreases (deficits) last from several minutes to several hours and have minor deviations. They are detected by ground-based plastic scintillation detectors with energy threshold above ~ 100 MeV. Most secondary cosmic rays of these energies reaching the Earth's surface are muons ($>65\%$) and gamma rays. Since the detection efficiency of gamma rays is significantly smaller than that of charged particles, the observed variations of count rate are caused mainly by muons.

While the enhancements of the fluxes have been successively modeled theoretically [9–14], the phenomenon of muon deficit has not been reasonably described yet. In Refs. [3–6], this problem is considered as the consequence of the change of energetic spectrum of muons influenced by the large potential difference between the ground and high altitudes where muons are born. However, the estimates are based on nonrealistic assumptions of very significant (several hundreds of MV) potential difference

between the ground level and altitudes 15–20 km. In reality, the thunderstorm fields, as a rule, have a layered structure with alternating field polarity (see, e.g., Refs. [15,16]) so that the net potential difference between the ground and the upper atmosphere does not surpass a few dozen MV. A more correct model was presented in Ref. [7] relating the decreasing muon flux to the life span of muons between the generation altitude at 15–20 km and the ground. In the presence of a decelerating electric field, the muons coming from the altitude where they were generated need a longer time to reach the surface detectors. As a result, the number of arriving muons decreases due to their decay. However, this model does not account for muon losses and the transformation of the muon energetic spectrum in the electric field. A comprehensive quantitative description of muon variations should include two mechanisms: (i) the transformation of an energetic spectrum of muons in the electric field and (ii) the decay of muons. In this paper, we develop an appropriate theoretical model based on these two mechanisms and derive the amplitude of variations at a given altitudinal profile of the electric field.

II. MUON FLUX IN THE ELECTRIC FIELD OF A THUNDERCLOUD

Suppose that a muon detector with energy threshold E_{th} is placed at altitude h_0 . The flux of muons hitting the detector and creating the counting rate contains muons coming from different altitudes where they are born.

The higher the altitude, the larger the muon's energy must be to reach the detector because of the ionization losses of muons traversing through the air (the bremsstrahlung and pair production losses of muons up to energies ~ 1000 GeV are negligibly small). The ionization losses of muons slightly grow along with the energy increase so that up to several GeV energies, they can be regarded as the constant quantity ~ 1.8 MeV/(g/cm²). Taking into account that the air density decreases with the altitude, as in $d_0 \exp(-kh)$, where $d_0 \sim 0.0012$ g/cm³ is the air density at sea level, h is the altitude above sea level in meters, and $k \sim 0.00013$ (1/m), one can express the ionization losses of the muon at the altitude h as $A \exp(-kh)$, where $A \sim 0.22$ (MeV/m). Thus, the muon experiences a drag force $A \exp(-kh)$ and an electric force from the electric field of the thundercloud when moving in the atmosphere during a thunderstorm. An appropriate equation governing the change of the energy of a vertically falling muon is written, therefore, as

$$\frac{dE}{dh} = A \exp(-kh) + ef(h), \quad (1)$$

where E is kinetic energy of the muon, $f(h)$ is the electric field depending of the altitude h , and e is the charge of the muon.

Note that in Eq. (1), the positive sign of the electric field corresponds to deceleration, and the negative sign corresponds to the acceleration of the muon.

Solving Eq. (1) for the muon having initial energy $E(h)$ at altitude h , we obtain the following expression for the energy of the muon at a lower altitude z conditioned by ionization losses:

$$E(z) = E(h) - \frac{A}{k} \left(\exp(-kz) - \exp(-kh) \right) - (V(h) - V(z)). \quad (2)$$

Here, the function $V(x)$ denotes the electric potential at the altitude x written as

$$V(x) = \int_0^x f(z) dz. \quad (3)$$

From Eq. (2), we introduce the ‘‘loss curve’’ $E_L(h)$ as the following:

$$E_L(h) = E(h_0) + \frac{A}{k} \left(\exp(-kh_0) - \exp(-kh) \right) + V(h) - V(h_0) \quad (4)$$

The loss curve determines energy $E_L(h)$ whose muon must have at the altitude h in order to reach the altitude h_0 with the energy $E(h_0)$. Index L indicates that the energy change takes place due to ionization losses.

Next, we have to take into account the decaying of muons. The life span of a nonrelativistic muon $\tau \sim 2.2 \mu\text{s}$ is, in fact, the average time between the muon's birth and its decaying. Some muons live shorter than τ , whereas others live longer. However, for simplicity, we will assume that the life span of all nonrelativistic muons is τ . For high energy muons, the life span increases due to the relativistic slowing of time. A muon with kinetic energy E will have a life span of $\gamma\tau$ ($\gamma = 1 + E/mc^2$ is the Lorentz factor, m is the muon mass, and c is the speed of light) so that the propagation length of the high energy muon $v\gamma\tau$ (v is the speed of the muon) increases and such a muon can travel several kilometers before decaying. Since the energy of the muon changes when traveling in the atmosphere, the Lorentz factor γ changes correspondingly. Therefore, in order to calculate the propagation length of a high energy muon, one must divide its trajectory into smaller parts, where the Lorentz factor γ is approximately constant and then sum (integrate) these parts. As a result, the following equation determining the propagation distance D of the muon with variable energy $E(z)$ along this path is obtained:

$$\begin{aligned} D &= \int_0^\tau v(t)\gamma(t) dt \\ &= \frac{1}{c} \int_0^{c\tau} v(z)\gamma(z) dz \\ &\sim \int_0^{c\tau} \gamma(z) dz \sim c\tau + \frac{1}{mc^2} \int_0^{c\tau} E(z) dz. \end{aligned} \quad (5)$$

Here we assume that the energy of the muon is larger than ~ 100 MeV, so that $v(z) > 0.8c \sim c$. Substituting in Eq. (5) the expression for $E(z)$ from Eq. (2), as well as $D = h - h_0$ and replacing the integration limits $c\tau \rightarrow h$, $0 \rightarrow (h - c\tau)$, we have

$$\begin{aligned} E(h) &= \frac{mc^2}{\tau} (h - h_0) - mc^2 \\ &+ \frac{A}{k^2 c \tau} \exp(-kh) \left(\exp(kc\tau) - kc\tau - 1 \right) \\ &- e \int_{h-c\tau}^h V(z) dz + ec\tau V(h). \end{aligned} \quad (6)$$

We will call the curve corresponding to this equation the ‘‘decaying curve’’ $E_D(h)$ by adding the index D , which means decaying. The decaying curve $E_D(h)$ determines the energy whose muon must have at the altitude h in order to reach the altitude h_0 just before decaying. Equation (6) can be simplified by expanding $\exp(kc\tau)$ in a Taylor series, as well as by integrating the potential by using Eq. (3) and changing the order of integration. After some transformations, we come to the following equation for the decaying curve:

$$\begin{aligned}
 E_D(h) = & \frac{mc}{\tau}(h - h_0) - mc^2 + \frac{Ac\tau}{2}\exp(-kh) \\
 & + e\left(V(h) - V(h - c\tau)\right) \\
 & + \frac{e}{c\tau} \int_{h-c\tau}^h (h-x)f(x)dx. \quad (7)
 \end{aligned}$$

In Fig. 1(a), both the loss and decaying curves calculated by Eqs. (2) and (7) in the absence of an electric field are plotted. Only the muons corresponding to the area above both curves can reach the altitude h_0 before decaying with energy larger than E_{th} and, therefore, to contribute to the counting rate of the detector with threshold energy E_{th} (we assume that the sensitivity of the detector does not depend on the energy of the muon).

In the presence of an electric field, these curves are transformed. For simplicity, let us first suppose that the electric field is constant and has the value 0.02 MV/m. When this field decelerates the muons, they must have larger energy to reach the altitude h_0 with energy E_{th} . Therefore, in the case of decelerating field, the loss curve goes up, and for the accelerating field, it is lower than in the absence of the electric field, as seen in Fig. 1(b). Analogously, the decaying curves in the presence of the electric field calculated by Eq. (7) are plotted; however, as seen in Fig. 1(b), the shifts of the decaying curve due to the electric field are significantly smaller. Thus, in the presence of the electric field, the graphical region of accelerated muons increases, whereas the region of decelerated muons decreases. These changes of integration regions lead to corresponding changes of the fluxes: the decrease of the flux of decelerated muons is determined by region 1 in Fig. 1(b), and the increase of the flux of accelerated muons

is determined by region 2. From Fig. 1(b), it is seen that region 1 is always larger than region 2. This is due to the specific mutual displacement of the loss and decaying curves, which means that a significant portion of the accelerated muons decay before reaching the altitude h_0 . It is seen that at altitudes above ~ 10000 m, the integration region is determined solely by the decaying curve, which slightly changes in the electric field. Therefore, the variations of muon flux near the ground are caused mainly by muons born at altitudes up to ~ 10000 m. Note that in the absence of the decaying curve for stable particles (e.g., electrons and positrons), the regions of the accelerated (decelerated) electrons and decelerated (accelerated) positrons are approximately equal. Therefore, no changes in the total flux of electrons + positrons will take place in the presence of an atmospheric electric field.

Thus, the above-introduced concept of loss and decaying curves provides a transparent method for the computation of muon flux in the presence of the electric field. To find the flux of muons, one should outline the loss and decaying curves for a given altitudinal profile of the electric field and then integrate a flux density by the energy and altitude in the region above both the loss and decaying curves.

Let us now compute these changes of muon fluxes. To do this, one needs to know the density function $F(E, h)$, which determines the flux of muons with energy E born at the altitude h . Note that this function differs from the well-known differential spectrum of muons $S(E, h)$. Indeed, $S(E, h)$ gives the flux of muons with energies E near altitude h ; it can be generated from convenient EXPACS software [17–19]. This flux is formed by muons born at all altitudes above h ; meanwhile, $F(E, h)$ is the flux of muons with energy E born near altitude h . Hence, we have the following equation connecting $S(E, h)$ and $F(E, h)$:

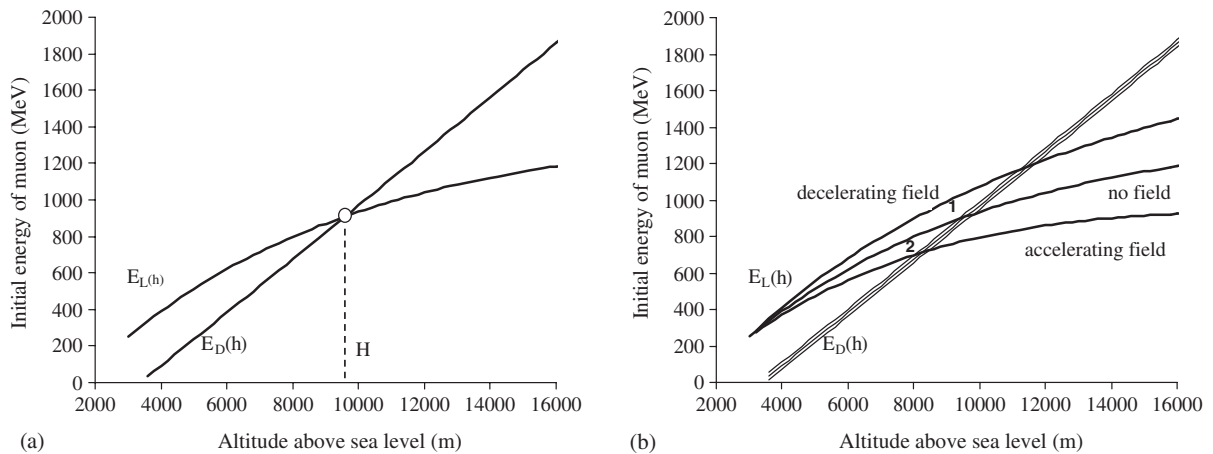


FIG. 1. The loss $E_L(h)$ and decaying $E_D(h)$ curves, determined by Eqs. (2) and (7) in the absence (a) and the presence (b) of uniform electric field 0.02 MV/m. Detector with threshold energy $E_{\text{th}} = 250$ MeV is placed at the altitude $h_0 = 3000$ m. $H \sim 9600$ m is intersection point of two curves. In (b) all three decaying curves, corresponding to accelerating, decelerating and non electric fields are close to each other. Region 1 determines the decrease of the flux of decelerated muons, whereas the region 2 determines the increase of the flux of accelerated muons.

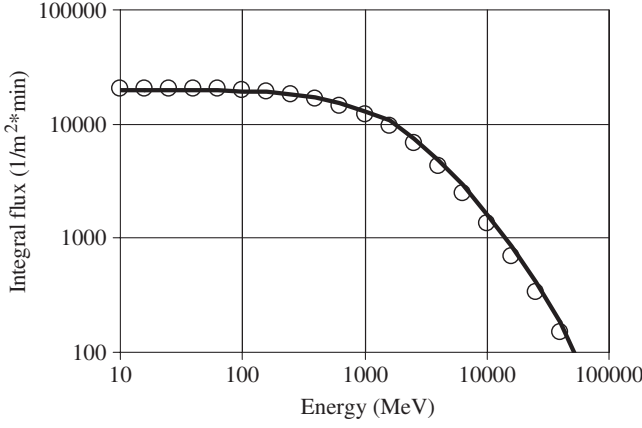


FIG. 2. Integral flux of muons at the altitude 3000 m in the absence of electric field, calculated by Eq. (9) (the solid line) and Eq. (8) with EXPACS data (open circles).

$$\begin{aligned}
 I(E, h_0) &= \int_E^\infty S(E', h_0) dE' = & (8) \\
 &= \left(\int_{h_0}^{H(E)} dh \int_{E_L(h)}^\infty dE' + \int_{H(E)}^\infty dh \int_{E_D(h)}^\infty dE' \right) \\
 &\quad \times F(E', h) & (9)
 \end{aligned}$$

Here, $I(E, h_0)$ is the integral flux of muons at altitude h_0 , which can be derived either by calculating the integral of the differential flux above energy E [Eq. (8)] or by calculating the integral of the density function above both E and h [Eq. (9)]. The integral in Eq. (9) is calculated above the loss curve for the altitudes $h < H(E)$ [$H(E)$ is the intersection point of the loss and decaying curves] and above the decaying curve for altitudes $h > H(E)$, as seen in Fig. 1(a). From Eqs. (8) and (9), one can assume that $F(E, h)$ can be approximated by the derivative of $S(E, h)$ by h , i.e., $F(E, h) \sim K \cdot dS(E, h)/dh$, where K is an unknown constant. Substituting this expression in Eq. (9) and calculating the integral, we obtain the integral flux

$I(E, h_0)$. The same flux is obtained by calculating the integral $S(E', h)$ according to Eq. (8).

The integration limits in Eqs. (8) and (9) are set to 20 km for h (the particle flux at higher altitudes is negligibly small) and 120 GeV for E (the integral flux of the muons with larger energies is $< 0.01\%$). The unknown constant K is found from the computation of the integral flux of muons by Eqs. (8) and (9). As a result, we obtain the value $K \sim 0.22$, for which Eqs. (8) and (9) give approximately the same value. In Fig. 2, both calculated integral fluxes when $K = 0.22$ are plotted. We see that the solid line representing Eq. (9) is very close to the real spectrum obtained from Eq. (8) by using EXPACS data. It confirms the correctness of Eq. (9) with density function $F(E, h)$ taken as

$$\begin{aligned}
 F(E, h) &= F_+(E, h) + F_-(E, h), \\
 F_+(E, h) &\sim 0.22 \frac{\partial S_+(E, h)}{\partial h}, \\
 F_-(E, h) &\sim 0.22 \frac{\partial S_-(E, h)}{\partial h}, & (10)
 \end{aligned}$$

where $S_+(E, h)$ and $S_-(E, h)$ are differential spectrums of positive and negative muons at altitude h .

Now we are able to calculate the flux of the muons at any given altitudinal profile of the electric field $f(h)$.

The experimental data [15,16] show that generally the electric field is upward directed in the lower layer of a thundercloud and downward directed in the upper layer (left panel in Fig. 3). However, opposite profiles of the electric field are observed as well (right panel in Fig. 3). The first configuration of the electric field (upward directed in the lower layer) we call below the upward field (UF), and the second configuration we call the downward field (DF). The UF corresponds to positive $f(h)$, whereas DF corresponds to negative $f(h)$. We will approximate the altitudinal profiles of the electric field by the pieces of linear functions. Then the profiles shown in the left and right panels in Fig. 3 are fitted by the functions $f(h)$ as the following:

$$f_{\text{UF}}(h) = \begin{cases} 0.15f_1 & \text{if } 0 < h < 4250 \text{ m} \\ f_1(h/1500 - 2.67) & \text{if } 4250 \text{ m} < h < 5500 \text{ m} \\ -f_1(h/1500 - 4.67) & \text{if } 5500 \text{ m} < h < 8500 \text{ m} \\ f_1(h/4500 - 2.89) & \text{if } 8500 \text{ m} < h < 13000 \text{ m} \\ f_1(h/1500 - 8.67) & \text{if } 13000 \text{ m} < h < 14000 \text{ m} \\ -f_1(h/1500 - 10) & \text{if } 14000 \text{ m} < h < 15000 \text{ m} \end{cases}, & (11)$$

$$f_{\text{DF}}(h) = \begin{cases} -f_2(h/4000 - 0.75) & \text{if } 3000 \text{ m} < h < 7000 \text{ m} \\ f_2(h/1000 - 8) & \text{if } 7000 \text{ m} < h < 9000 \text{ m} \\ -f_2(h/3000 - 4) & \text{if } 9000 \text{ m} < h < 12000 \text{ m} \end{cases}, & (12)$$

where $f_1 \sim 75$ kV/m, $f_2 \sim 50$ kV/m

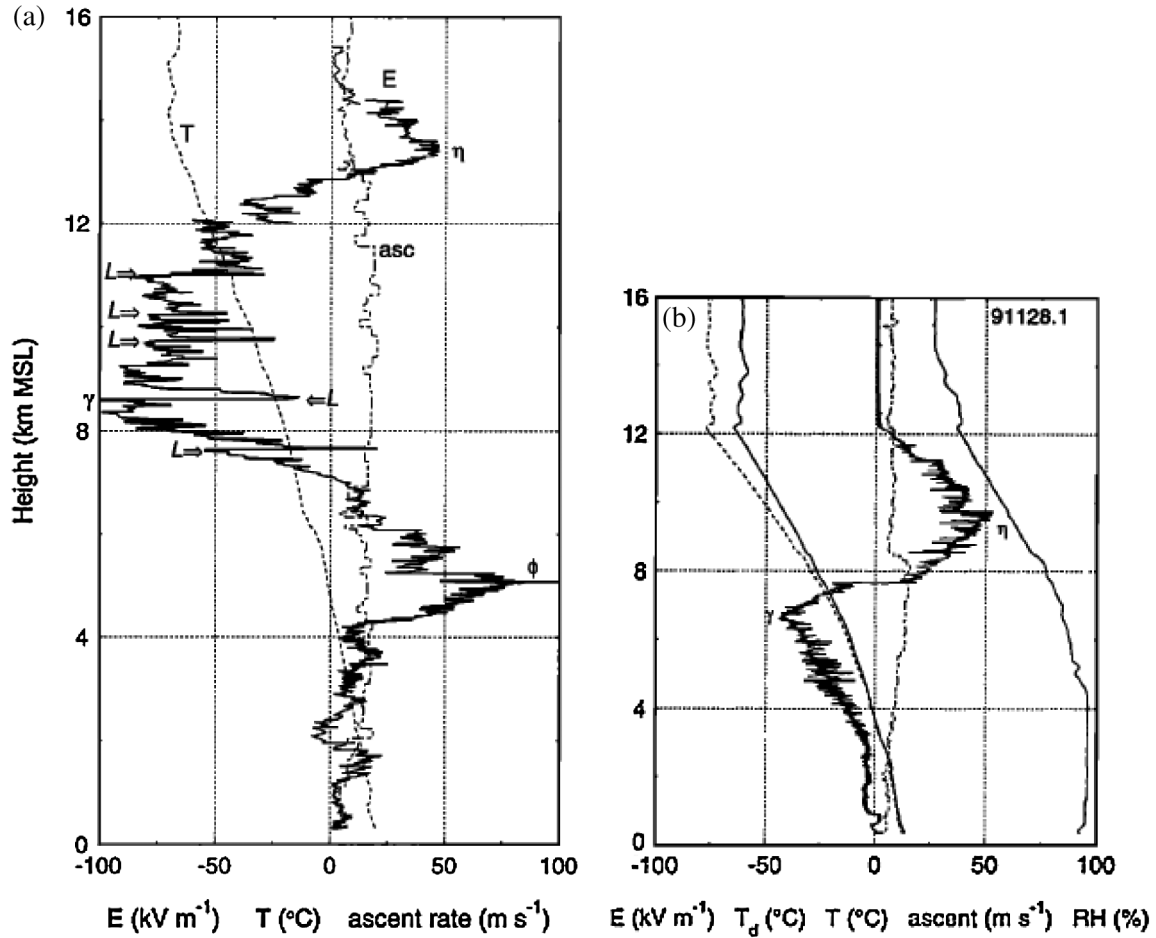


FIG. 3. Different altitudinal profiles of electric field, measured in balloon experiments from [16]. Left panel: UF–upward directed electric field in lower layer ($h \sim 4000 \text{ m} - 6500 \text{ m}$) and downward directed in the upper layer ($h \sim 6500 \text{ m} - 13000 \text{ m}$). Right panel: DF–downward directed in the lower layer ($h \sim 3500 \text{ m} - 7500 \text{ m}$) and upward directed in the upper layer ($h \sim 7500 \text{ m} - 12000 \text{ m}$). The curves are electric field E (thin solid lines), temperature T (dotted lines), dew point temperature T_d (thick solid line in the right panel), the ascent rate of the balloon (dashed lines), and relative humidity with respect to water RH (thick solid line in the right panel).

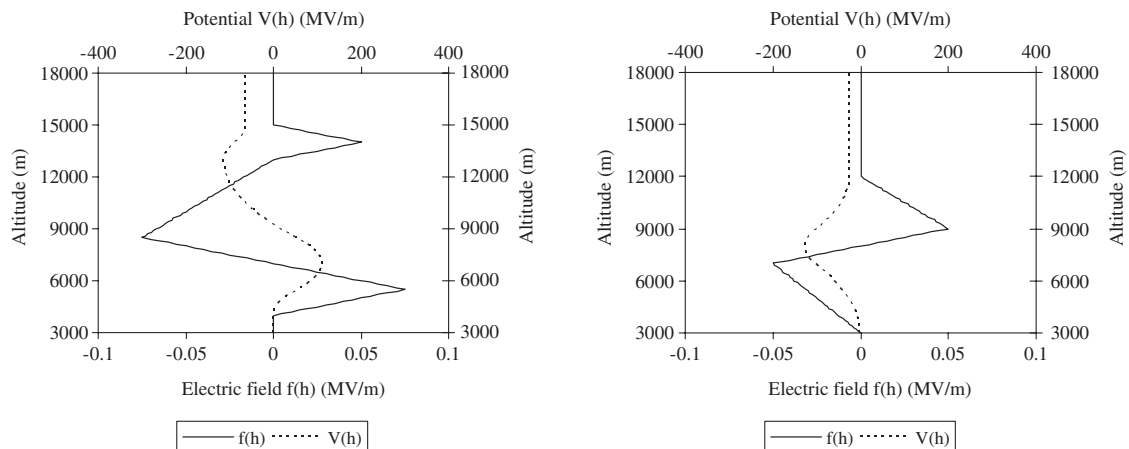


FIG. 4. Electric field $f(h)$ and potential $V(h)$ versus the altitude, calculated by the Eqs. (11), (12), and (3) with $f_1 \sim 0.075 \text{ MV/m}$, $f_2 \sim 0.05 \text{ MV/m}$ (potential of the ground is set 0).

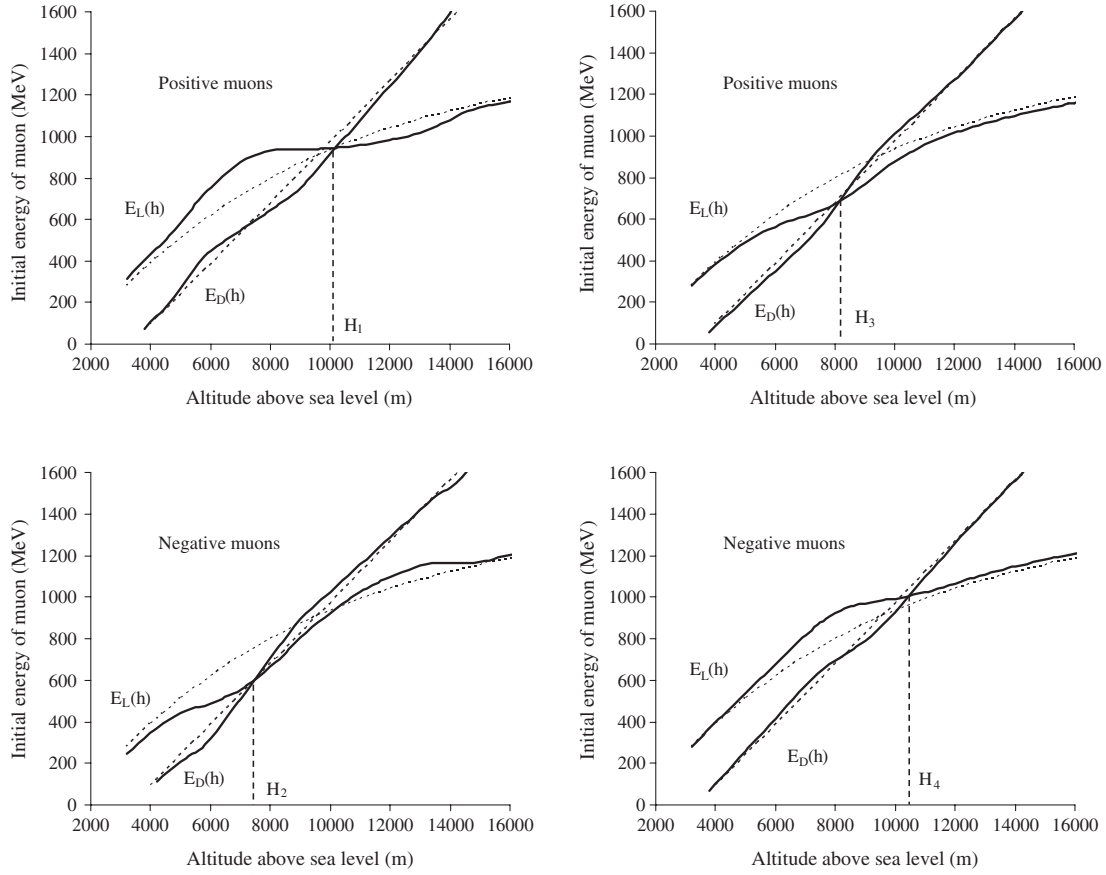


FIG. 5. The loss $E_L(h)$ and decaying $E_D(h)$ curves of muons for the UF and DF given by Eqs. (11) (left panels) and (12) (right panels). The dotted lines represent the loss and decaying curves in the absence of electric field. The altitudes of intersection points are $H_1 \sim 10200$ m, $H_2 \sim 7500$ m, $H_3 \sim 8100$ m, and $H_4 \sim 10400$ m. Detector with threshold energy $E_{th} = 250$ MeV is placed at the altitude $h_0 = 3000$ m.

Function $f(h)$ and potential $V(h)$ calculated by Eqs. (11) and (12) are presented in Fig. 4. It is seen that the electric potential inside the clouds gets the value up to ~ 170 MV; however, at higher altitudes, it decreases to ~ 20 -40 MV.

Having $f(h)$ and $V(h)$, we calculate the loss and decaying curves by Eqs. (2) and (7) for $E_{th} = 250$ MeV and $h_0 = 3000$ m presented in Fig. 5. A flux of positive I_{p+} and negative I_{m-} muons for the UF is computed by the integration of function $F_+(E, h)$ [Eq. (10)] in the region above both the loss and decaying curves as follows:

$$I_{m+} = \left(\int_{3000}^{H_1} dh \int_{E_L(h)}^{120000} dE + \int_{H_1}^{20000} dh \int_{E_D(h)}^{120000} dE \right) F_+(E, h), \quad (13)$$

$$I_{m-} = \left(\int_{3000}^{H_2} dh \int_{E_L(h)}^{120000} dE + \int_{H_2}^{20000} dh \int_{E_D(h)}^{120000} dE \right) F_-(E, h). \quad (14)$$

The total flux of muons I_{tot} and the percentage change of total flux d are, therefore,

$$I_{tot} = I_{m+} + I_{m-}, \quad (15)$$

$$d = 100 \frac{I_{tot} - I(E_{th}, h_0)}{I(E_{th}, h_0)}. \quad (16)$$

Here, $I(E_{th}, h_0) \sim 19500$ ($1/m^2 * min$) is the integral flux of the positive and negative muons with energies larger than about 250 MeV at altitude $h_0 \sim 3000$ m in the absence of an electric field. It is calculated by Eqs. (9) or (10) by using EXPACS data for the differential spectrum of muons and contains roughly 10700 ($1/m^2 * min$) positive and 8800 ($1/m^2 * min$) negative muons.

Analogously, the muon flux is calculated for the DF given by Eq. (12),

$$I_{m+} = \left(\int_{3000}^{H_3} dh \int_{E_L(h)}^{120000} dE + \int_{H_3}^{20000} dh \int_{E_D(h)}^{120000} dE \right) F_+(E, h), \quad (17)$$

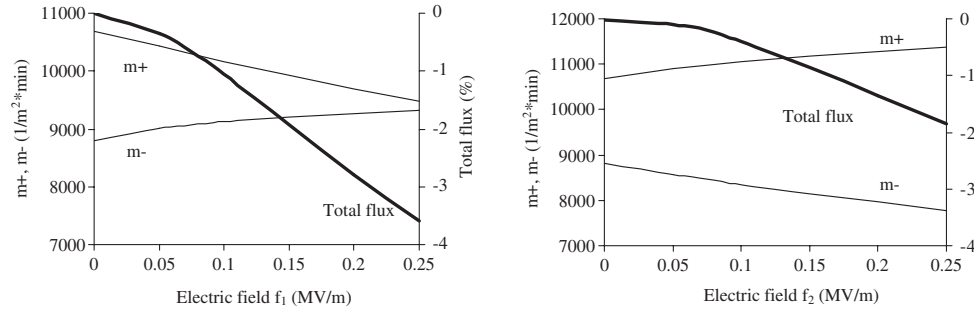


FIG. 6. Integral fluxes of positive (m^+), negative (m^-) and total muons versus the amplitude of electric field in the lower layer of thundercloud for the UF given by Eq. (11) (the left panel) and the DF given by Eq. (12) (the right panel). Detector with threshold energy $E_{th} = 250$ MeV is placed at the altitude $h_0 = 3000$ m.

$$I_{m^-} = \left(\int_{3000}^{H_4} dh \int_{E_L(h)}^{120000} dE + \int_{H_4}^{20000} dh \int_{E_D(h)}^{120000} dE \right) F_-(E, h). \quad (18)$$

The calculations of Eqs. (13)–(18) give in both cases the negative changes $d \sim -0.6\%$ and $d \sim -0.1\%$. Since the electric field inside the thundercloud can get larger than the considered 0.075 and 0.05 MV/m values, let us change f_1 and f_2 in Eqs. (11) and (12) and investigate muon fluxes at larger amplitudes of the electric field with the same profile. The calculations yield the graphs in Fig. 6.

We see that in the case of UF, the flux of the positive muons decreases and the flux of the negative muons increases, whereas in the case of DW, it is vice versa. In both cases, the decrease of the fluxes is conditioned by the deceleration of muons, which leads to the lift of the loss curves. The corresponding increase of the fluxes of negative (for UF) and positive (for DF) muons is smaller, due to the decaying of some portion of these muons.

Thus, for the aforementioned two opposite profiles of the electric field, the flux of the muons with energy >250 MeV

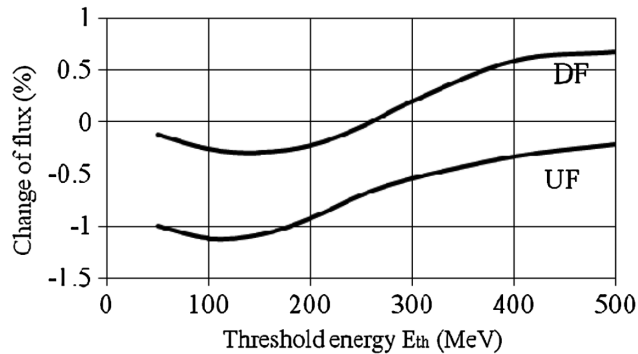


FIG. 7. The change of the count rate versus threshold energy of the detector, placed at the altitude 3000 m in case of the UF, given by Eq. (11) and the DF, given by Eq. (12).

at altitude 3000 m decreases. Note, however, that since the loss curve depends on the threshold energy of the detector, one should expect different changes of muon flux measured by detectors with different energy thresholds. Particularly, for large E_{th} , the loss curve can lift the upper decaying curve so that the integration regions in Eqs. (13), (14), (17), and (18) will be determined by only the loss curve. In such circumstances, the essential factors are the abundance of positive muons compared to negative muons and the net potential difference between the ground and upper atmosphere. Consequently, the count rate of a detector with a large threshold can be either negative or positive. In the special profiles given by Eqs. (11) and (12), these variations versus the threshold energy of the detector are presented in Fig. 7. The analogous curves can be derived for other special profiles of the electric field.

In conclusion, we developed the concept of the loss and decaying curves to investigate variations of muon flux near the ground during thunderstorms. It turns out that mainly muons born at altitudes up to ~ 10000 m are responsible for this phenomenon. We showed that the variations emerge due to the collective action of two processes: (i) the acceleration/deceleration of muons determined by the loss curve and (ii) the decay of muons determined by the decaying curve. These variations are either negative or positive, depending on the profile of the electric field and the threshold energy of the detector. Generally (i.e., in case of UF), the flux of positive muons decreases in the lower layer of a thundercloud, whereas a corresponding increase of the flux of negative muons is limited by their partial decaying. As a result, an uncompensated decrease in the total flux of muons near the ground emerges, which can be observed by detectors with any threshold energy. In case of DF, the same process is responsible for decreasing the total flux of muons registered by the detector with threshold energy up to ~ 300 MeV. However, at higher energy threshold, the process of decaying does not play any role, and the change of flux is determined by the acceleration/deceleration of muons only. In such case, the abundance of positive muons relative to negative muons and the net

potential difference between the ground and upper atmosphere become the key factors. As a result, the flux of muons detected by a detector with higher energy threshold may increase in case of DF.

ACKNOWLEDGMENTS

The work was partially supported by the ISTC Grant No. 1554.

-
- [1] J. R. Dwyer, D. M. Smith, and S. A. Cummer, *Space Sci. Rev.* **173**, 133 (2012).
- [2] V. V. Alexeenko *et al.*, in *Proceedings of the 20th International Cosmic Ray Conference, Moscow* (Nauka, Moscow, 1987), Vol. **4**, pp. 272–275.
- [3] L. I. Dorman and I. V. Dorman, in *Proceedings of the 24th International Cosmic Ray Conference, Rome* (Editrice Compositori, Bologna, 1995), Vol. **4**, pp. 1160–1163.
- [4] L. I. Dorman, *Cosmic Rays in the Earth's Atmosphere and Underground* (Kluwer Academic Publishers, Dordrecht, 2004).
- [5] P. V. Mironychev, *Geomagn. Aeron.* **43**, 654 (2003).
- [6] Y. Muraki *et al.*, *Phys. Rev. D* **69**, 123010 (2004).
- [7] N. S. Khaerdinov and A. S. Lidvansky, and V. B. Petkov, in *Proceedings of the 29th International Cosmic Ray Conference, Pune, 2005* (Tata Institute of Fundamental Research, Mumbai, 2005), Vol. **2**, pp. 389–392.
- [8] A. S. Lidvansky and N. S. Khaerdinov, *Bull. Russ. Acad. Sci. Phys.* **73**, 397 (2009).
- [9] A. V. Gurevich, G. M. Milikh, and R. Roussel-Dupre, *Phys. Lett. A* **165**, 463 (1992).
- [10] R. A. Roussel-Dupré, A. V. Gurevich, T. Tunnell, and G. M. Milikh, *Phys. Rev. E* **49**, 2257 (1994).
- [11] A. V. Gurevich and K. P. Zybin, *Phys. Usp.* **44**, 1119 (2001).
- [12] L. P. Babich, R. I. Ilkaev, I. M. Kutsyk, A. Yu. Kudryavtsev, R. A. Roussel-Dupre, and E. M. Symbalysty, *Geomagn. Aeron.* **44**, 243 (2004).
- [13] J. R. Dwyer, *Phys. Plasma* **14**, 042901 (2007).
- [14] G. G. Karapetyan, *Astropart. Phys.* **38**, 46 (2012).
- [15] T. C. Marshall, W. Rison, W. David Rust, M. Stolzenburg, J. C. Willett, and W. P. Winn, *J. Geophys. Res.* **100**, 20815 (1995).
- [16] M. Stolzenburg, W. David Rust, B. F. Smull, and T. C. Marshall, *J. Geophys. Res.* **103**, 14059 (1998).
- [17] T. Sato and K. Niita, *Radiat. Res.* **166**, 544 (2006).
- [18] T. Sato, H. Yasuda, K. Niita, A. Endo, and L. Sihver, *Radiat. Res.* **170**, 244 (2008).
- [19] <http://phits.jaea.go.jp/expacs/>.